J. Fluid Mech. (2014), *vol.* 747, *pp.* 635–655.
doi:10.1017/jfm.2014.171

Multifractality in combustion noise: predicting an impending combustion instability

Vineeth Nair and R. I. Sujith†

Department of Aerospace Engineering, Indian Institute of Technology Madras, Chennai-600036, India

(Received 22 April 2013; revised 24 January 2014; accepted 26 March 2014;
first published online 23 April 2014)

The transition in dynamics from low-amplitude, aperiodic, combustion noise to high-amplitude, periodic, combustion instability in confined, combustion environments was studied experimentally in a laboratory-scale combustor with two different flameholding devices in a turbulent flow field. We show that the low-amplitude, irregular pressure fluctuations acquired during stable regimes, termed 'combustion noise', display scale invariance and have a multifractal signature that disappears at the onset of combustion instability. Traditional analysis often treats combustion noise and combustion instability as acoustic problems wherein the irregular fluctuations observed in experiments are often considered as a stochastic background to the dynamics. We demonstrate that the irregular fluctuations contain useful information of prognostic value by defining representative measures such as Hurst exponents that can act as early warning signals to impending instability in fielded combustors.

Key words: fractals, turbulent reacting flows, wave–turbulence interactions

1. Background

Unsteady combustion of a turbulent, convecting air–fuel mixture tends to be noisy, even more so when the heat release happens in a confined space (Strahle 1978). These fluctuations can at times get amplified, when localized hydrodynamic perturbations augmented by the heat release couple with the acoustics of the chamber – resulting in self-sustained, large-amplitude pressure oscillations termed as combustion instability (McManus, Poinsot & Candel 1993). Such oscillations are often detrimental and cause losses in billions of dollars of annual revenue to gas-turbine manufacturers. For instance, the repair and replacement costs of hot-section components due to combustion instability alone exceeds $1 billion annually and amounts to approximately 70 % of the non-fuel costs of F class gas turbines (Lieuwen & Yang 2005). Designers of high-energy propulsion and power generation systems have hence resorted to conservative stability margins as a preventive measure. Setting such conservative and often experience-based operational boundaries results in increased levels of NO_x emissions, which makes it difficult for gas-turbine manufacturers to meet the stringent emission norms. In propulsion devices such as rockets and ramjets, one may not even have the flexibility of choosing such a conservative, stable operational boundary. Despite decades of active research, an understanding of the mechanisms underlying this transition is far from complete and

† Email address for correspondence: sujith@iitm.ac.in

finding robust precursors that can forewarn impending combustion instability remains an important practical problem.

The topics of combustion noise and combustion instability both figure fairly prominently in the combustion literature (see for example Strahle 1978; McManus *et al.* 1993; Candel 2002; Culick 2006; Candel *et al.* 2009; Schwarz & Janicka 2009 for extensive reviews on the topics). However, most studies individually assess and contrast stable and unstable operation in combustors; studies that perform a smooth variation of operating parameters starting from stable operation, leading towards instability remain few. Thus, although various physical mechanisms responsible for combustion instability have been identified from earlier studies, the exact nature of transition, or the pathways (routes) through which instability is established is still not well understood. Chakravarthy and co-workers (Chakravarthy *et al.* 2007; Chakravarthy, Sivakumar & Shreenivasan 2007) performed a systematic variation of operating conditions in bluff-body and backward-facing step combustors from stable to unstable operation. They reported that the non-lock-on regime (where vortex shedding and duct acoustics do not lock-on) is characterized by low-amplitude broadband noise generation. However, at the onset of lock-on (between vortex shedding and duct acoustics), the broadband noise generation gives way to the excitation of high-amplitude discrete tones, which could be limit-cycle oscillations. Recently, Gotoda *et al.* (2011) have presented results from an experimental investigation on the onset of thermoacoustic oscillations for decreases in the fuel equivalence ratio. The study employed novel methods of nonlinear time series analysis and reported the possibility of encountering low-dimensional chaotic oscillations in combustors.

The sources of combustion noise should be deterministic, as they derive from various fluid dynamic and combustion processes: flame roll-up, vortex coalescence or impingement, fluid dilatation etc. (Coats 1996), which are governed by a deterministic set of equations. In a recent study, the pressure measurements acquired during stable operation in combustors (combustion noise) was rigorously shown to be deterministic chaos (Nair *et al.* 2013) using techniques from dynamical systems theory. Further, they showed that a loss of this chaotic behaviour could act as an early warning as operating conditions approach combustion instability. The use of the term 'noise' to describe the phenomena, therefore, creates confusion, since the measured signals (as will be shown later) do not display any properties one would expect from an uncorrelated noisy signal (such as zero memory of past events).

However, combustion noise is typically modelled as an acoustic problem by decoupling the hydrodynamics from the analysis. In a review by Candel *et al.* (2009), the authors clearly describe the formulation and its drawbacks as follows: '*Studies of combustion noise generally focus on situations where the flow dynamics can be considered to be independent of the radiated sound. It is implicitly assumed that the flow dynamics is decoupled from the induced wave motion and the sound emission from unstable flames is generally not considered when dealing with combustion noise*'. As they further note, such a decoupling – although it could ease computations – cannot be justified because practical systems are confined and boundaries reflect sound towards the reactive region. In summary, there exists a gap between the ways in which combustion noise is understood and theoretically modelled.

Combustion instability is also fundamentally treated as an acoustic problem and the effects of turbulence are often times decoupled or neglected (Lieuwen 2001, 2002, 2003; Noiray & Schuermans 2013). The traditional approach in dealing with unsteady measurements acquired from combustors is to treat these measurements as signals modulated by random perturbations. In models, turbulence is introduced as

an external perturbation to the wave equation – as random inputs or inputs with the properties determined by the measured power spectrum (Clavin, Kim & Williams 1994; Burnley & Culick 2000; Lieuwen & Banaszuk 2005 to mention a few). In such a mean-field description, the spectrum of dynamics under consideration is restricted to fixed points and limit-cycle oscillations, wherein the observed amplitude modulations in the measured data are described as the effects of background noise. The strategy then is to identify conditions of linear instability of the system, the boundaries of which form the margins of operability of the combustor. Despite the progress made in the modelling of combustion instabilities, there still exists considerable difficulty in the prediction of the operating conditions under which the system loses stability (Lieuwen & Yang 2005). This limitation is possibly a consequence of the traditional 'signal plus noise' paradigm assumed in the analysis of such oscillations. Since it is possible that the irregular fluctuations seen in measurements are a direct result of the inherent complexity of turbulent combustion dynamics, it is unclear whether a separation of the measurements into a signal and noise is justified.

From a more practical viewpoint, an important additional question is to know whether we can extract information about an impending instability from these fluctuations. Most of the stability detection and control schemes in combustors focus on detecting an incipient instability; for instance, by monitoring the r.m.s. levels of pressure fluctuations or the peak pressure amplitude in the Fourier transformed pressure signal. Such measures detect an instability only after it has begun, at which stage it may be too late to take adequate control action to save the combustor from wear and tear and possible mechanical failure. To resolve this question on precursors, we propose a formalism which involves searching for precursors to instability in data acquired from turbulent combustion environments, for conditions ranging from low-amplitude combustion noise to high-amplitude combustion-driven oscillations. That the formalism is data driven should be seen as an advantage, because models or simulations often contain many inherent assumptions themselves. Further, suitable models can be appropriately devised once the underlying mechanisms are well understood. The existence of precursors would imply that it is possible, at least in principle, to reconstruct the dynamics that generates low-amplitude combustion noise. Identifying precursors – at the very least – should provide operators of fielded combustion systems with sufficient warning of impending oscillations.

One way to obtain early warning measures is to force the system under consideration with broadband noise (Wiesenfeld 1985; Surovyatkina 2005). The noise gets selectively amplified at the instability frequencies when the operating conditions are sufficiently close to instability. The width of the frequency peak in the amplitude spectrum then informs of the proximity of the system to instability (Wiesenfeld 1985). Further, it has also been observed that there is a reduction in the width of the bistable regime for systems exhibiting subcritical bifurcation when the levels of noise used to force the system are increased (Surovyatkina 2005). However, it should be noted that this procedure involves external stochastic forcing of a deterministic system; our interests lie in describing the deterministic features of the system itself. Moreover, the dynamics of a forced system is different from that of a self-evolving system, especially with regards to the phase of the resulting oscillations (Pikovsky, Rosenblum & Kurths 2001) and the transient envelope of the growing oscillations (Burnley & Culick 2000; Culick 2006). Also, introducing noise can lead to noise-induced transitions (Jegadeesan & Sujith 2013), with dynamics different from that of the original system. It is well known that a system with chaotic dynamics can result in signals that appear noisy. Hence, a word of caution is in order before summarily classifying combustion noise as stochastic or deterministic.

A chaotic time signal can be identified through its self-similar structure, resulting in patterns that fill non-integer dimensions called fractals. A fractal time series has sections that resemble the whole and hence can be distinguished from stochastic signals, which are – by definition – devoid of any patterns. The non-integer dimension of occupation of a fractal is termed the fractal dimension. A multifractal time series differs from a fractal series in that it is composed of interwoven subsets with different fractal dimensions (Frisch & Parisi 1985). Gouldin was the first to recognize the utility of applying fractal geometry concepts to combustion problems in both turbulent premixed and diffusion flames (Gouldin 1987; Gouldin, Hilton & Lamb 1988; Gouldin, Bray & Chen 1989). However, most of these and several subsequent studies focused on the geometrical aspects of open flames. Using hot-film anemometry of the cold flow and Rayleigh scattering density measurements, multifractality in the time series data of turbulent premixed open flames was illustrated by Strahle & Jagoda (1988). However, the utility of the fractal description to measurements made in confined combusting environments has not been explored, save for a recent study on the pressure fluctuations acquired prior to lean blowout (Gotoda *et al.* 2012).

Since a multifractal process entails multiple time scales, it must necessarily display a broad spectrum in the frequency domain, such as one would observe in turbulent velocity measurements. It is now well known that turbulent velocity measures are multifractal (Sreenivasan & Meneveau 1986; Meneveau & Sreenivasan 1987; Prasad, Meneveau & Sreenivasan 1988; Sreenivasan & Meneveau 1988; Meneveau & Sreenivasan 1989, 1991 to name a few pioneering studies; see Sreenivasan 1991 for an excellent review on the subject). Energy injected into a turbulent flow at large scales cascades down multiplicatively through the inertial subrange down to Kolmogorov scales, where it is finally dissipated. The multifractal formalism is necessary to understand and explain the reason for the intermittency observed in the measurements of this energy dissipation rate in the inertial range.

The amplitude spectrum of ducted combustion noise is also known have a broad profile in the frequency domain, with shallow peaks in the vicinity of acoustic modes of the duct (Chakravarthy *et al.* 2007). It would therefore be interesting to examine whether measured pressure fluctuations acquired during such stable operating conditions in combustors are amenable to a multifractal description. We know that the transition to combustion instability results in a transition of the spectrum, from a broad one with shallow peaks, to one with sharp, discrete peaks. Provided combustion noise is multifractal, we should therefore expect deviations from this multifractality when the operating conditions are varied systematically towards combustion instability. Such deviations – if they exist – are of prognostic value, since they presage an impending instability. The solution to the original question of identifying precursors to combustion instability hence can be answered by identifying whether combustion noise is multifractal or not.

The paper is organized as follows. A brief overview of the multifractal formalism and multiplicative processes is presented in § 2. In § 3, we describe experiments performed to investigate multifractality in combustion noise, the results of which are discussed in § 4. The key findings are then summarized in § 5. Finally, details on the computation of multifractal measures from a given time series are elaborated in the Appendix.

2. Multifractal formalism

The term ‘fractal’ is used to describe objects that have a fractional dimension (Mandelbrot 1982). Whereas classical Euclidean geometry deals with smooth objects

that have integer dimensions, structures in nature often tend to be fractals because they are wrinkly at all levels of magnification. Measures such as length, area or volume cannot be defined for such objects since they depend on the scale of measurement. For instance, the length of a fractal curve increases when the ruler is made smaller because additional details are now revealed. A logarithmic plot of the measured length of the curve against the length of the ruler for such a curve would then show an inverse power law; i.e. a straight line with a negative slope. This slope, which is a number between one and two, is referred to as the 'fractal dimension' of the curve. Thus, we see that such curves occupy more space than a straight line, which scales as the length of the ruler, but less space than a square, which scales as the square of the length of the ruler.

The concept of fractals can also be used to describe complex dynamics that results in fluctuations spread over multiple orders of temporal magnitude. A fractal process is characterized by a broadband power spectrum with an inverse power law, known more popularly as the $1/f$ spectrum (Montroll & Schlesinger 1982; Schlesinger 1987) since there is here an inverse relationship between frequency and power. Similar to a fractal curve, a fractal time signal also has a dimension between one and two. A fractal time series also displays a property known as 'scale invariance', which means that features of the signal look the same on many different scales of observation (seconds, minutes etc.). Mathematically, for a fractal time signal, $p(ct) = p(t)/c^H$ for some scaling c and a constant H. Scale invariance thus relates the time series across multiple time scales. Such a dependence on multiple time scales results in a broad profile of responses in the amplitude spectrum, representative of details that are present at these time scales. Conversely, if the process can adequately be represented in terms of one or a few discrete time scales, then the signal would have an amplitude spectrum with discrete, narrow peaks. In the next subsection, we will show how the presence of fractality is related to the memory of a time signal.

2.1. *Statistical description of a time signal*

Statistical analysis of time signals involve obtaining the distribution of their fluctuations (Gaussian, Poisson, Levy etc.) or representing this distribution in terms of representative measures computed around the most likely measurement value (central moments). Fluctuations that are fractals, but appear noise-like, differ from noise in that they do not satisfy the statistics of classical random variables. Whereas the central moments of a random variable are bounded in time, the central moments of a fractal signal diverge with time, at least over a short range (Mandelbrot 1974). This can happen – for instance – when the measurement values represent variations both in time and space, which makes the signal non-stationary. A signal is non-stationary if the central moments vary with time or, in other words, there is a variation in the underlying distribution of data values. As an example, unsteady pressure values acquired during confined combustion in a convecting flow field are non-stationary, since the pressure measurement at any location at a given instant depends not only on pressure values at previous instants, but also on the pressure values at other locations in the flow field.

In the description of non-stationary time signals, classical measures such as mean or variance are not very useful since they vary with time. Instead, they are characterized by examining how the moments depend on the time interval over which they are evaluated. For instance, the dependency of the standard deviation of the time signal on the time interval is encapsulated in a parameter called the Hurst exponent H

(Hurst 1951). It measures the amount of correlation or the memory in a time series and is related to the fractal dimension D of the time series as $D = 2 - H$ (Bassingthwaighte, Liebovitch & West 1994).The concept of structure functions introduced by Kolmogorov (Kolmogorov 1941; Frisch 1995) is a generalized version of this idea, which explores scaling relationships between the variations in the moments of measured fluctuations and the time interval of measurement.

A time series is called persistent (anti-correlated) if a large value is typically (i.e. with high statistical preference) followed by a large value and a small value is followed by a small value (Kantelhardt 2011). In other words, the signal retains a memory of what happened in the previous time step and has an increased probability of the next step being in the same direction – such signals have a trend. For a persistent signal, the Hurst exponent H lies between 0.5 and 1 and the strength of the trend increases as H approaches 1. An anti-persistent (correlated) time series, on the other hand, is one in which a large value is typically followed by a small value, and a small value is followed by a large value. Such signals have a tendency to revert to their mean value. For anti-persistent signals, values of H lie between 0 and 0.5. The strength of mean reversion increases as H approaches 0. For time signals that are persistent or anti-persistent, the fractal scaling law holds in at least a limited range of scales (Kantelhardt 2011). For an uncorrelated time series, the Hurst exponent is 0.5. This is expected, since the variance of fluctuations in a memory-less diffusion process should scale linearly with time.

The Hurst exponent also determines the scaling properties of the fractal time series. If $p(t)$ is a fractal time signal with Hurst exponent H, then $p(ct) = p(t)/c^H$ is another fractal signal with the same statistics (West *et al.* 2003). Algorithms that compute the Hurst exponent are mostly based on this scaling property. This scaling behaviour typically has upper and lower cutoffs that are dependent on the system dynamics. Detrended fluctuation analysis (DFA) (Peng *et al.* 1994) provides an easy approach to characterize fractality in a given time series data. Through an evaluation of the structure functions, correlations in the data are sought for by computing the Hurst exponent, which can then be related to the fractal dimension of the time series.

2.2. *Multifractality and multiplicative processes*

Many time signals exhibit a complex scaling behaviour that cannot be accounted for by a single fractal dimension. A full description of the scaling in such signals involves multiple generalized Hurst exponents, resulting in interwoven subsets of varying fractal dimension (varying Hurst exponents) producing what is termed a 'multifractal' behaviour (Frisch & Parisi 1985). In other words, fluctuations in a time signal that have different amplitudes follow different scaling rules. The method of DFA can be expanded to explore multifractality in a time signal and the technique is called multifractal DFA (Kantelhardt *et al.* 2001, 2002). The procedure involves computing generalized Hurst exponents that describe the scaling of central moments that have been appropriately scaled for various negative as well as positive orders (q). For instance, standard deviation has an order of two and its scaling with time interval gives the Hurst exponent H^2 (hereafter referred to as H). For a multifractal signal the generalized Hurst exponents H^q would have different values for different q. Through a Legendre transform, this variation in generalized Hurst exponents at different orders can alternately be represented as a spectrum of singularities $f(\alpha)$, in terms of a new variable α which is conjugate to q. A plot of $f(\alpha)$ for various values of α is termed the multifractal spectrum, the width of which provides a measure of

the multifractality in the signal (see the Appendix for details on implementation). An excellent description of multifractal processes may be found in Paladin & Vulpiani (1987).

The presence of multifractality is an indication that there are multiplicative processes involved in the transfer of energy across various time scales (Sreenivasan 1991). Provided one accepts Taylor's frozen-flow hypothesis (Taylor 1938), the argument can be extended to hold for energy transfer across various spatial scales as well. The energy transfer at turbulent flow conditions involves a multiplicative Richardson's cascade (Richardson 1922) in the inertial subrange from the integral scale down to the Kolmogorov scale. As a consequence of this cascade, we should expect the multifractality to persist even in the presence of heat addition. However, the onset of combustion instability transforms the dynamics from one characterized by a multiplicity of scales to one dominated by a few discrete time scales associated with the formation of large-scale coherent structures in the flow field. It remains an interesting problem to identify how the interaction of turbulence with the acoustic field of a confinement transforms such an energy transfer across multiple time scales to transfers that are dominated by a few time scales. This can happen – for instance – through an inverse cascade (Kraichnan 1967), wherein the energy of the smaller scales gets transferred to progressively larger scales. The formation of large-scale coherent structures during combustion instability possibly hints at the presence of such an inverse cascade co-existing simultaneously with the usual direct cascade that dissipates energy at Kolmogorov scales.

3. Experiments

Experiments were performed on a combustor with two different flame-holding mechanisms: a fixed-vane swirler, and a circular bluff body, at high Reynolds numbers ($Re > 16\,000$). Schematics of the set-up and the flame-holding devices are shown in figure 1. It consists of a plenum chamber, a burner and a combustion chamber with extension ducts. The burner was provided with a central shaft of diameter 16 mm to support the bluff body or the fixed-vane swirler. The swirler consists of eight blades with a vane angle of 40° and was positioned at the exit of the burner with a centre body for flame stabilization. The centre body was located such that its edge is in the exit plane of the burner. For the experiments involving flame stabilization using a bluff body, the swirler was replaced by a circular disk of diameter 47 mm and thickness 10 mm. The bluff body was located at a fixed position of 50 mm from the rearward facing step using a rack and pinion traverse that has a least count of 1 mm. A disk of 2 mm thickness with 300 holes of diameter 1.7 mm was located 30 mm downstream of the fuel-injection location to act as a flashback arrestor. The combustion chamber consists of a sudden expansion from the circular burner of diameter 40 mm into a square geometry of cross-section 90×90 mm^2. The length of the combustor chamber along with the extension ducts was set at 700 mm and pressure transducers were mounted at different locations along this length. A spark plug with a step-up transformer was mounted in the dump plane for ignition of the fuel–air mixture. A blow-down mechanism was used to supply air from high-pressure tanks, which then passed through a moisture separator before finally entering the plenum chamber. The central shaft was also used to deliver the fuel into the chamber through four radial injection holes of diameter 1.7 mm. The fuel was injected 100 mm upstream of the rear end of the swirler and 160 mm upstream of the rear end of the bluff body.

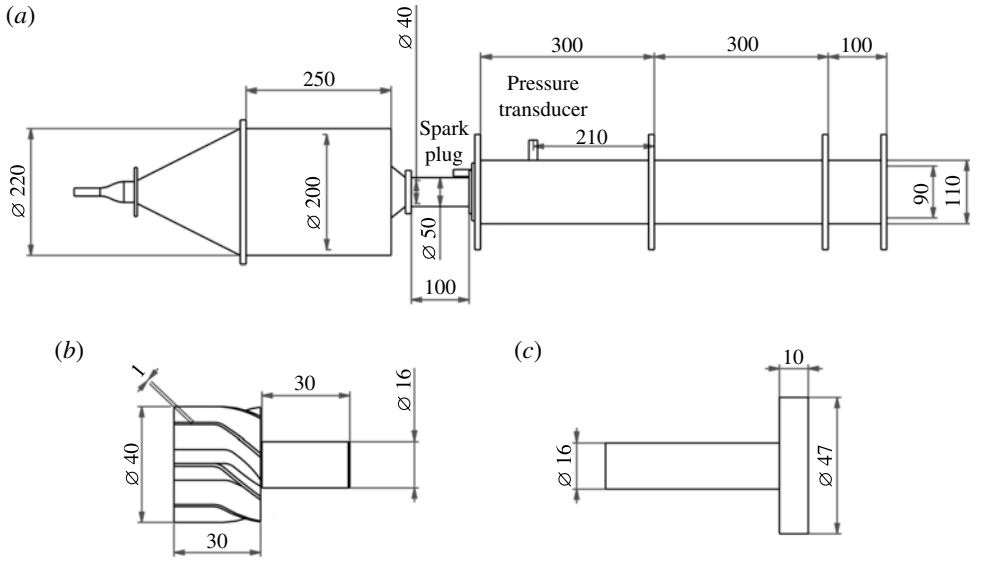

FIGURE 1. (*a*) The experimental set-up used in the current study. The two flame-holding mechanisms used were: (*b*) a fixed-vane swirler, and (*c*) a circular bluff body. Fuel is injected through four radial holes using the central shaft and spark-ignited using an 11 kV ignition transformer. The length of the combustion chamber is 700 mm, with three extension ducts, two of length 300 mm and one of length 100 mm. The swirler turns the flow by 40° at its exit plane. The design of the combustor was adapted from Komarek & Polifke (2010).

To accurately control and measure the air-flow rates ($\dot{m}_a$) and the fuel-flow rates ($\dot{m}_f$), mass flow controllers with digital logging and monitoring capabilities (Alicat Scientific, MCR Series) were used which had an uncertainty of ± (0.8 % of reading +0.2 % of full scale). Unsteady pressure measurements (p') reported in this study were acquired 90 mm from the rearward facing step using a piezoelectric transducer (sensitivity 72.5 mV kPa^{-1}, 0.48 Pa resolution and ±0.64 % uncertainty) mounted on a specially fabricated pressure port flush-mounted on the combustor wall. A Teflon adapter was used to protect the transducer from excess heating and the mount was provided with semi-infinite tubes (6 m in length) to ensure integrity in the measured signals. The phase correction required with this arrangement was calculated to be less than 2°. The voltage signals from the pressure transducer were acquired using a 16-bit A–D conversion card (NI-643) with an input voltage range of ±5 V and a resolution of ±0.15 mV.

For all the experiments conducted, the ambient temperature was measured to be (27 ± 1) °C using a dry bulb thermometer and the relative humidity was measured to be (85 ± 1) % on a hygrometer. The measurements made by the mass flow controllers were in standard litres per minute (standardized for air at 25 °C, 14.696 psi) which was then converted to g s^{-1} for computing the Reynolds number (*Re*). The fuel used was LPG which is 60 % C_4H_{10} and 40 % C_3H_8 by volume. The Reynolds number was obtained as $Re = 4\dot{m}D_1/\pi\mu D_0^2$, where $\dot{m}(= \dot{m}_a + \dot{m}_f)$ is the mass-flow rate of the fuel–air mixture, D_0 is the diameter of the burner, D_1 is diameter of the circular bluff body (for experiments with the swirler, $D_1 = D_0$) and μ is the dynamic viscosity of the fuel–air mixture at the experimental conditions. In the calculation of *Re*,

corrections to viscosity were made for changes in the fuel–air ratio, the procedure for which can be found in Wilke (1950).

To ensure that the ambient conditions did not change between the experiments, the decay rates of the acoustic field in the combustion chamber were measured multiple times prior to combustion by forcing the combustors with a loudspeaker placed at the exit of the chamber at the fundamental acoustic frequency – 133 Hz for the swirl-stabilized combustor and 135 Hz for the bluff-body-stabilized combustor. The decay rate was then obtained as the slope of a semi-log plot of the amplitude decay with time when the forcing was switched off. These decay rates had an average value of $-37\ \mathrm{s}^{-1}$ with a variation of less than 3 % even after accounting for the change of configuration from swirler to bluff body.

The measurements were acquired keeping the fuel-flow rate fixed and progressively increasing the air-flow rates. When the air-flow rate increases for a fixed fuel-flow rate, the equivalence ratio (ϕ) decreases bringing the combustion towards the lean regime. It is well known that lean combustion in a confinement is prone to large amplitude instabilities (Candel 2002). Recent experiments on pipe tones reveal that, even in the absence of combustion, an increase in Reynolds number can transition a chaotic turbulent state towards periodic states (Nair & Sujith 2013). Hence, the control parameter in the experiments performed was chosen as Re to identify similarities in the transition from chaotic to periodic oscillations in various systems with turbulent flow-sound interaction.

4. Results

The pressure measurements acquired from the two flame-holding configurations during stable operation and after the onset of combustion instability are shown in figure 2. The fluctuations prior to instability (figure 2*a*,*c*) are seemingly random and display an amplitude spectrum which is broadband (figure 2*e*). This has traditionally been classified as combustion noise in the literature. After the onset, the amplitude spectrum has sharp, discrete peaks (figure 2*f*) distinctive of combustion instability. The amplitudes of these oscillations are fairly high (figure 2*b*,*d*) compared to combustion noise, suggesting an underlying lock-in mechanism. Such a lock-in may happen, for instance, between the hydrodynamic fluctuations associated with periodic vortex formation and the fluctuations of the acoustics in the confinement. It should be mentioned that although the spectrum of the signal prior to instability (figure 2*e*) has a shallow peak near the instability frequency, no information can be gleaned as to how close the operating conditions are to combustion instability, or which of the many frequencies that have comparable peaks in the spectrum would be the dominant frequency at instability. Therefore, the fractal properties of signals are sought to obtain precursors to combustion instability, by computing the Hurst exponents.

In order to demonstrate the utility of Hurst exponents in identifying the dynamics, a comparison is made of four different time series data: (i) Gaussian white noise ($\mathcal{N}(0,\ 1)$), (ii) combustion noise acquired from the swirl-stabilized configuration ($\phi = 1.0, Re = 1.6 \times 10^4$), (iii) combustion noise acquired from a bluff-body-stabilized configuration ($\phi = 1.1, Re = 1.8 \times 10^4$), and (iv) synthetic periodic data. The periodic data along with Gaussian white noise represent the limiting cases on the value of H for an anti-persistent (correlated) signal. The instability frequencies for the two flameholding configurations for the data presented at combustion instability (figure 2*b*,*d*) are 253.6 Hz (swirl) and 249 Hz (bluff body), respectively. Hence, the time scales for the computation of the Hurst exponent were varied between 8

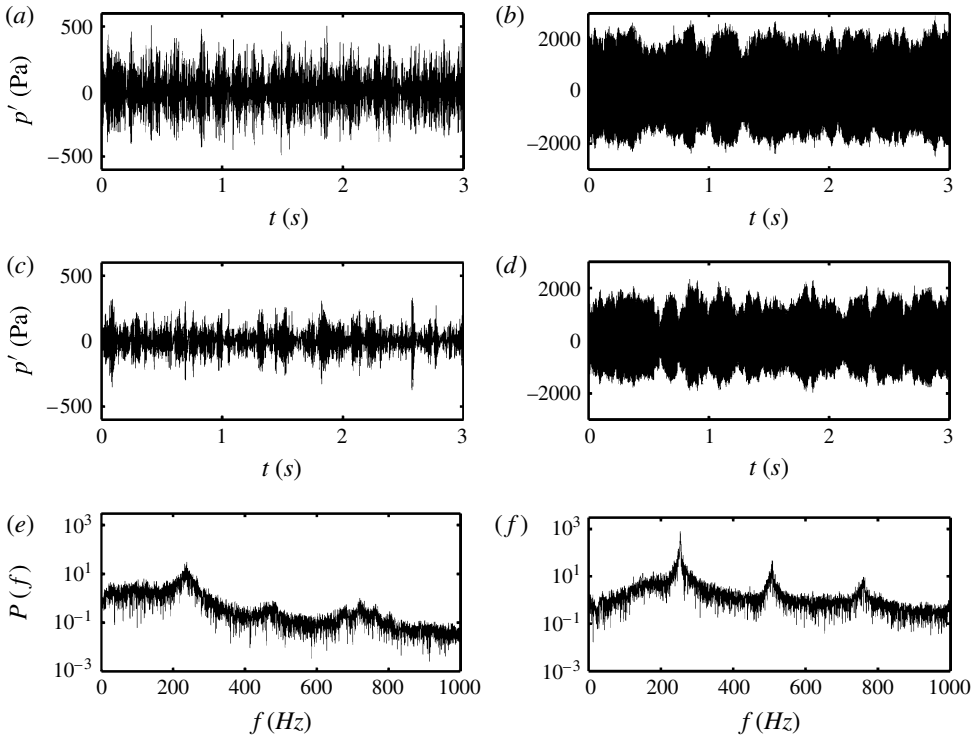

FIGURE 2. Unsteady pressure signals acquired from the swirl-stabilized configuration (*a*) $\phi = 1.0$, $Re = 1.6 \times 10^4$, (*b*) $\phi = 0.7$, $Re = 2.2 \times 10^4$ and the bluff-body-stabilized configuration (*c*) $\phi = 1.1$, $Re = 1.8 \times 10^4$, (*d*) $\phi = 0.7$, $Re = 2.8 \times 10^4$, showing transition from combustion noise to combustion instability. The transition in the amplitude spectrum from (*e*) a broad profile with shallow peaks to (*f*) the spectrum with sharp peaks as Re is varied towards combustion instability for the data from swirl-stabilized combustor. The bin size of frequency in calculating the FFT was 0.3 Hz. A similar transition is also observed in the bluff-body-stabilized configuration.

and 16 ms, which correspond approximately to two to four cycles of oscillations at combustion instability. For the sake of comparison, the frequency of the synthetic periodic data was chosen as 250 Hz so as to be in the vicinity of the dominant frequency of the data presented at combustion instability.

The Hurst exponent (H) was estimated for the four time signals as the slope of the variation of the structure function of these signals (F_w^2, see the Appendix for the details on the estimation of H) at different time scales of measurement (w) (shown in figure 3). White noise has a Hurst exponent of 0.5, characteristic of a diffusive Brownian process. This is because the variance scales linearly with time for white noise. Hence, the variation of the standard deviation with time, which is also the Hurst exponent, would have a slope of 0.5 when plotted on a logarithmic scale. The periodic data has a slope close to zero because the variance of the fluctuations must necessarily be bounded and remain constant over a time period. The slopes of the combustion noise data for both the configurations, however, lie between the two limiting conditions. Combustion noise thus represents an anti-persistent (correlated) fractal signal, since H is between 0 and 0.5. The fractal dimension D for such a signal lies between 1.5 and 2. The Hurst exponents obtained for the pressure signals

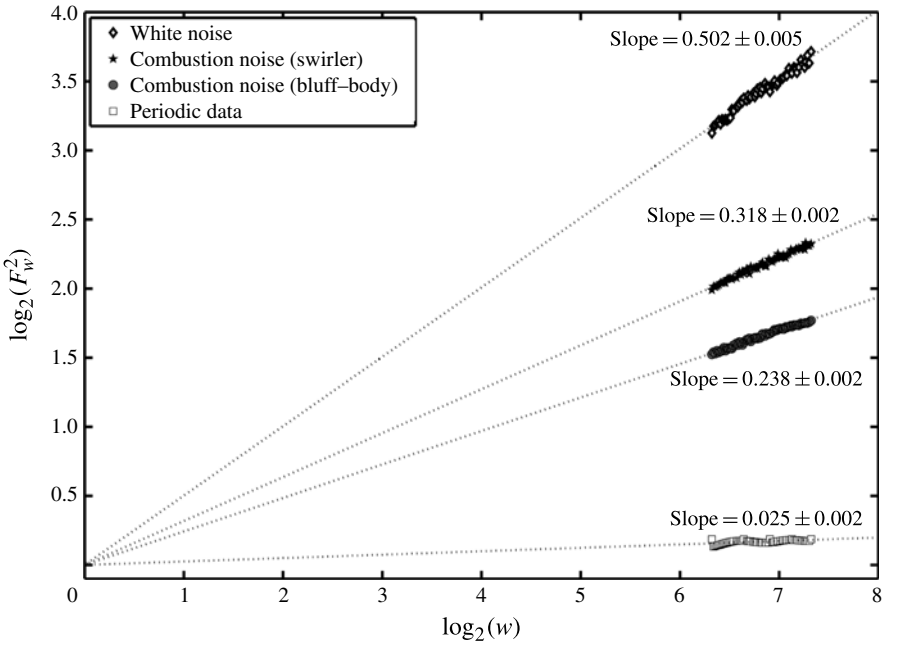

FIGURE 3. Illustration of fractal features of combustion noise through the Hurst exponent. The slopes of the curves represent the Hurst exponent H^2. The Hurst exponent for combustion noise has a slope that lies amidst those corresponding to Gaussian white noise and periodic oscillations. The intercepts have been removed from the abscissae and dotted lines are provided to guide the eye. Uncertainties reported correspond to standard errors in slope estimation.

at combustion instability (figure 2*b*,*d*) for the swirler and bluff body were 0.027 and 0.029 respectively, and are not shown in the plot for the sake of clarity.

The multifractality of the four signals presented in figure 3 was investigated by estimating the generalized Hurst exponents H^q, the results of which are shown in figure 4. The high- and low-amplitude fluctuations in different time intervals (w) are preferentially selected by varying the order of the structure function (q). Whereas a positive order ($q > 0$) selects high-amplitude fluctuations, a negative order ($q < 0$) would select low-amplitude fluctuations. The variation of the structure functions (F_w^q) with the size of the time interval are parallel for Gaussian white noise, with a slope of 0.5. This invariance of the slope with a value of 0.5 means that the fluctuations are uncorrelated at all amplitudes, and that F_w^q has an identical linear variation with time interval at all orders. For the periodic data, the values of H^q lie fairly close to zero at different q because there is just a single time scale associated with the fluctuations, which makes F_w^q bounded in time.

Now if combustion noise were monofractal; i.e. characterized by just a single fractal dimension, the time series should show a behaviour similar to that of white noise (figure 4*a*) with the same value for all the generalized Hurst exponents, albeit with a slope different from 0.5. However, for combustion noise, we see a difference in the slope of F^q at different values of q (figure 4*b*,*c*). This variation in the value of Hurst exponent H^q with q is a direct consequence of the multifractal nature of the time series (Kantelhardt 2011). The high- and low-amplitude fluctuations present in the time series scale differently, which results in different values of H^q at different q.

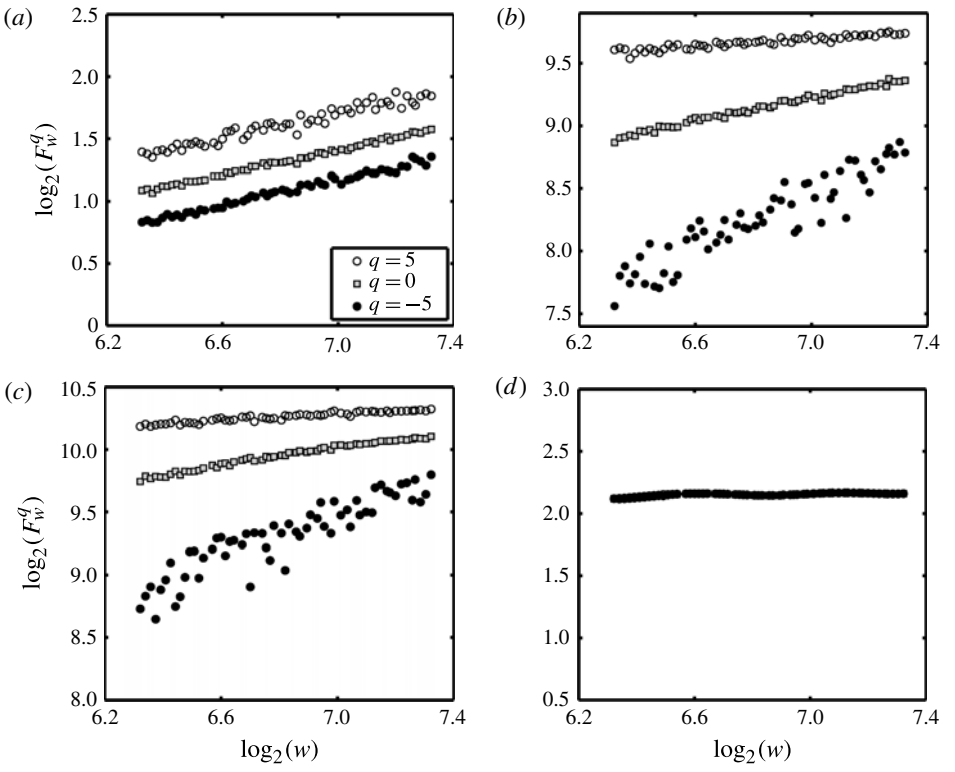

FIGURE 4. The variation in structure functions F_w^q at different orders q as the time interval w is increased (marked as hollow circles (○) for $q = 5$, squares (□) for $q = 0$, and filled circles (●) for $q = -5$). The data presented correspond to: (*a*) Gaussian white noise, (*b*) combustion noise from the swirl-stabilized configuration ($\phi = 1.0$, $Re = 1.6 \times 10^4$), (*c*) combustion noise from the bluff-body-stabilized configuration ($\phi = 1.1$, $Re = 1.8 \times 10^4$), and (*d*) synthetic periodic data ($f = 250$ Hz). The frequency of the synthetic data was chosen to be in the vicinity of the frequency at instability for the two configurations of the combustor ($f = 253.6$ Hz with the swirler and $f = 249$ Hz with the bluff body). The ordinates are shown on the same scale to represent the variations more clearly. The slope of the various curves give the generalized Hurst exponents H^q for that order q. The slopes for white noise and periodic data have values of 0.5 and 0 respectively for all F_w^q. Pressure signals acquired during combustion noise, on the other hand, have different slopes for different F_w^q.

The multifractal spectrum of these signals is shown in figure 5. The spectrum is broad for combustion noise whereas it is clustered around a point for the white noise and periodic data. For white noise, we see that the spectrum is concentrated around a value of 0.5, as expected. The clustering is around 0 for the periodic data, which indicates the absence of scale invariance for periodic time signals, because fluctuations happen only at one time scale.

Multifractality in a time series can come about in two ways: (i) due to a broad probability distribution of the data points, e.g. a Levy distribution, and (ii) due to different long-term correlations of the small- and large-scale fluctuations (Kantelhardt *et al.* 2002). An easy way to identify the presence of correlations in a time signal is to randomly shuffle its data values (West 2006). Whereas multifractality due to

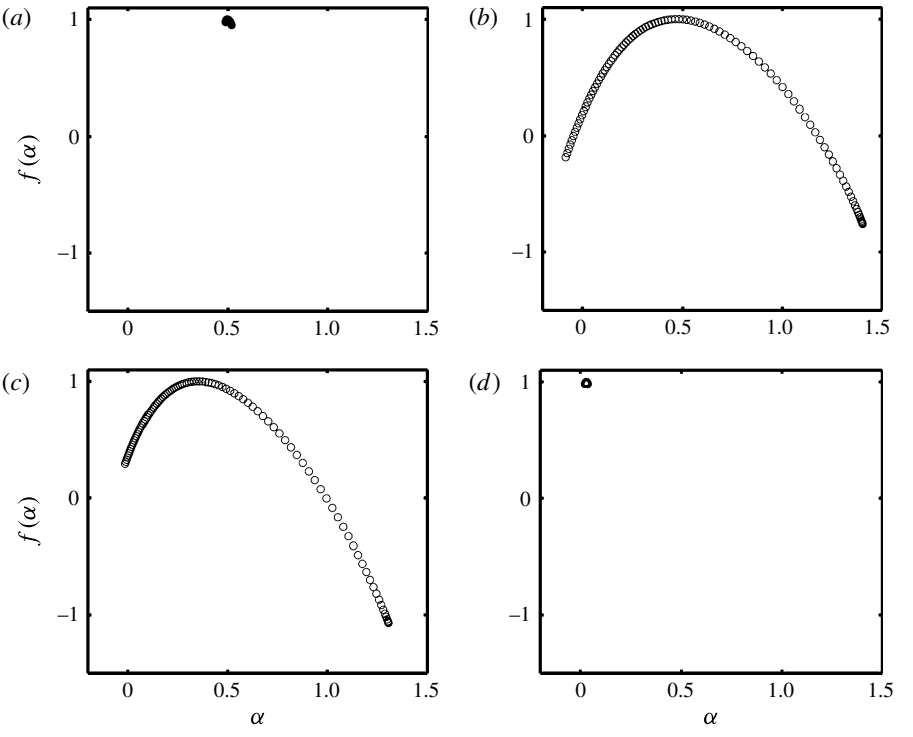

FIGURE 5. Multifractal analysis of different signals wherein the singularity spectrum $f(\alpha)$ is plotted as a function of the singularity strength α, which is comparable to the Hurst exponent. The data presented correspond to: (*a*) Gaussian white noise, (*b*) combustion noise from the swirl-stabilized configuration ($\phi = 1.0, Re = 1.6 \times 10^4$), (*c*) combustion noise from the bluff-body-stabilized configuration ($\phi = 1.1$, $Re = 1.8 \times 10^4$), and (*d*) synthetic periodic data. The spectrum for white noise and periodic data collapse to single points with singularity exponents 0.5 and 0 respectively, whereas it is broad for combustion noise.

correlations is removed by randomly shuffling the series, it persists in the former case even after shuffling. It is interesting to note that even when the multifractality arises due to long-term correlations, the probability density function of the time signal over a finite, fixed sampling duration can be a regular distribution with finite moments (for instance, a Gaussian). It is only when the sampling duration is varied that one observes the non-stationarity of the signal and divergence in central moments.

The source of multifractality in the data acquired during combustion noise was explored by randomly shuffling the acquired data as per the procedure suggested by West (2006). The original and the randomly shuffled surrogate pressure time series from the bluff-body-stabilized configuration are shown in figure 6(*a*,*b*). A zoomed-in view of the first 500 points in the series is shown in the inset. Whereas weak correlations are visible in combustion noise data, any such correlations are lost on randomly shuffling the data, making it memory-less. The distribution of the combustion noise data and the surrogate data is shown as a histogram in figure 6(*c*). The distribution naturally remains invariant on shuffling the data values. The distribution was verified to be Gaussian using the Kolmogorov–Smirnov test for normality (Massey 1951), with the null hypothesis for non-Gaussianity rejected at 5 % significance. This shows that even when the distribution of the acquired samples

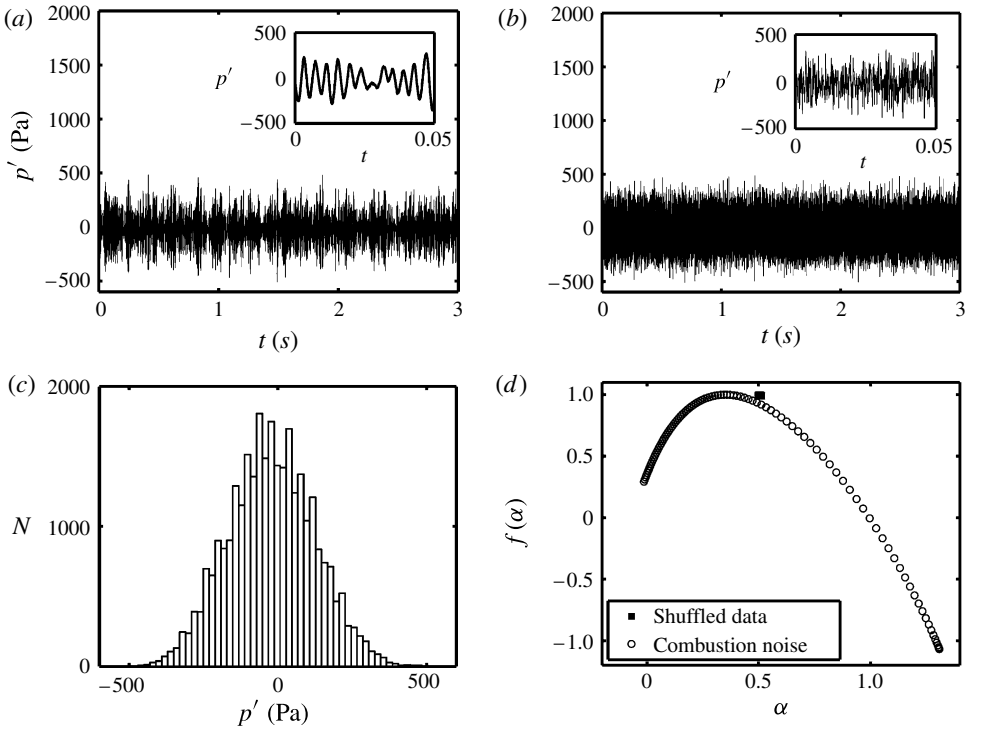

FIGURE 6. Effects of random shuffling on the combustion noise data ($\phi = 1.1, Re = 1.8 \times 10^4$) acquired from the bluff-body-stabilized configuration. Time signals of (*a*) the original data and (*b*) the randomly shuffled data. The first 500 points in both data sets are shown in the inset. Whereas combustion noise displays correlations with weak periodicity, the shuffled data is truly random, with no memory. (*c*) Histogram showing the distribution of the data points (N) in the two signals over 3 s. (*d*) Multifractal spectra for the original and randomly shuffled data. There is a loss of multifractality on randomly shuffling the data corresponding to combustion noise because of a loss of memory among the data points in the signal.

is a Gaussian, the dynamics can be complex and multifractal. The mere presence of correlations in the measured data suggests that it is incorrect to term the associated phenomena as 'combustion noise'. As shown in Nair *et al.* (2013), fluctuations termed combustion noise are chaotic and are the result of deterministic dynamics of the global system comprising flow, combustion and the chamber acoustics. In other words, combustion noise is deterministic chaos. It is probably the random appearance and the Gaussian distribution of the measured pressure fluctuations that prompted researchers to adopt a signal plus noise paradigm in analysing the combustion noise. To illustrate this point more clearly, the multifractal spectrum of the combustion noise and the shuffled series is shown in figure 6(*d*). Whereas the generalized Hurst exponents show variation at different orders, as illustrated by the broad spectrum, they are clustered around 0.5 for the shuffled data, indicating that it has degenerated into a noise-like data. Thus, we feel that a more suitable term to describe the phenomena is combustion chaos rather than combustion noise. In studying combustion noise and its transition to combustion instability, it may hence be imprudent to adopt the traditional signal plus noise paradigm, which currently is often implicitly assumed. Although

techniques such as computation of the fast Fourier transform (FFT) or obtaining the probability density function may suggest a noise-like behaviour, analysis using nonlinear fractal analysis can help discern deterministic features in measured signals, if present.

According to a conjecture by Kraichnan (1967), if energy is injected into the flow at a constant rate at some intermediate scale, an inverse cascade will take place until the largest scales available are attained. The process of combustion instability involves a periodic heat release rate, wherein the fluctuations in heat release rate are in a proper phase relationship with the perturbations in the acoustic pressure field thereby satisfying Rayleigh's criterion (Rayleigh 1878), which is a necessary condition for self-sustained pressure oscillations. The shear layer in a turbulent flow is characterized by several instability frequencies, corresponding to the different sizes of vortices (Winant & Browand 1974). On the interaction of acoustic waves with the shear layer, the vortex size can be stabilized when the frequencies of these waves match the instability frequencies of the shear layer (Schadow & Gutmark 1992). Hence, we suspect that the formation of large-scale coherent vortices at the onset of combustion instability, as reported in the literature (Rogers & Marble 1956; Parker, Sawyer & Ganji 1979; Pitz & Daily 1983; Smith & Zukoski 1985; Hegde *et al.* 1987; Poinsot *et al.* 1987; Yu, Trouve & Daily 1991 to name a few), is due to the establishment of an inverse cascade, with the energy being injected into the flow through combustion at scales defined by matching of the acoustics with the instability frequencies of the shear layer. Further, a theoretical analysis of nearly incompressible flows in the presence of heat addition (Zank & Matthaeus 1990) indicates the possibility of such an inverse cascade, wherein energy can get transported to the long-wavelength acoustic modes from smaller scales, provided the Mach numbers are low.

We have managed to successfully predict and prevent combustion instability in the two combustor configurations using the Hurst exponent H as an early warning measure (Nair *et al.* 2012); the results from the studies without control are shown in figure 7. The amplitude levels of the unsteady pressure fluctuations in the combustor are also presented for the sake of comparison in figure 7(*a*,*b*). The measures correspond to the r.m.s. values of the pressure fluctuations over the sampling interval (p_{rms}), as well as the peak amplitude at the dominant frequency obtained on taking the Fourier transform of the pressure signal (p_{FFT}), which are plotted as a function of Re. These amplitude measures capture an incipient instability; since the amplitudes rise only when the combustor actually becomes unstable, such measures inform an operator only that an instability has happened, not that it is going to occur.

The corresponding variation in the Hurst exponent for the two combustors is shown in figure 7(*c*,*d*). As Re is increased, there is smooth decrease in the value of H towards zero. This decrease happens well before the amplitude starts rising in the combustor. Hence, by defining a suitable threshold for H sufficiently distant from zero (say, 0.1), we can track the proximity of the system to instability and take suitable control measures. The results present the average value of H computed over segments ranging from roughly two to four acoustic cycles of the unsteady pressure data (8–16 ms) acquired over 3 s at a sampling rate of 10 kHz. However, it is possible to obtain comparable results even with shorter time signals. Also, the threshold is independent of the system configuration, since it merely is an indicator of the proximity of the system to an oscillatory regime.

The loss of multifractality in the signals at the onset of combustion instability is illustrated in figure 7(*e*,*f*). The plot clearly shows the spectrum $f(\alpha)$ diminishing to a point at the onset of combustion instability. This loss of multifractality happens

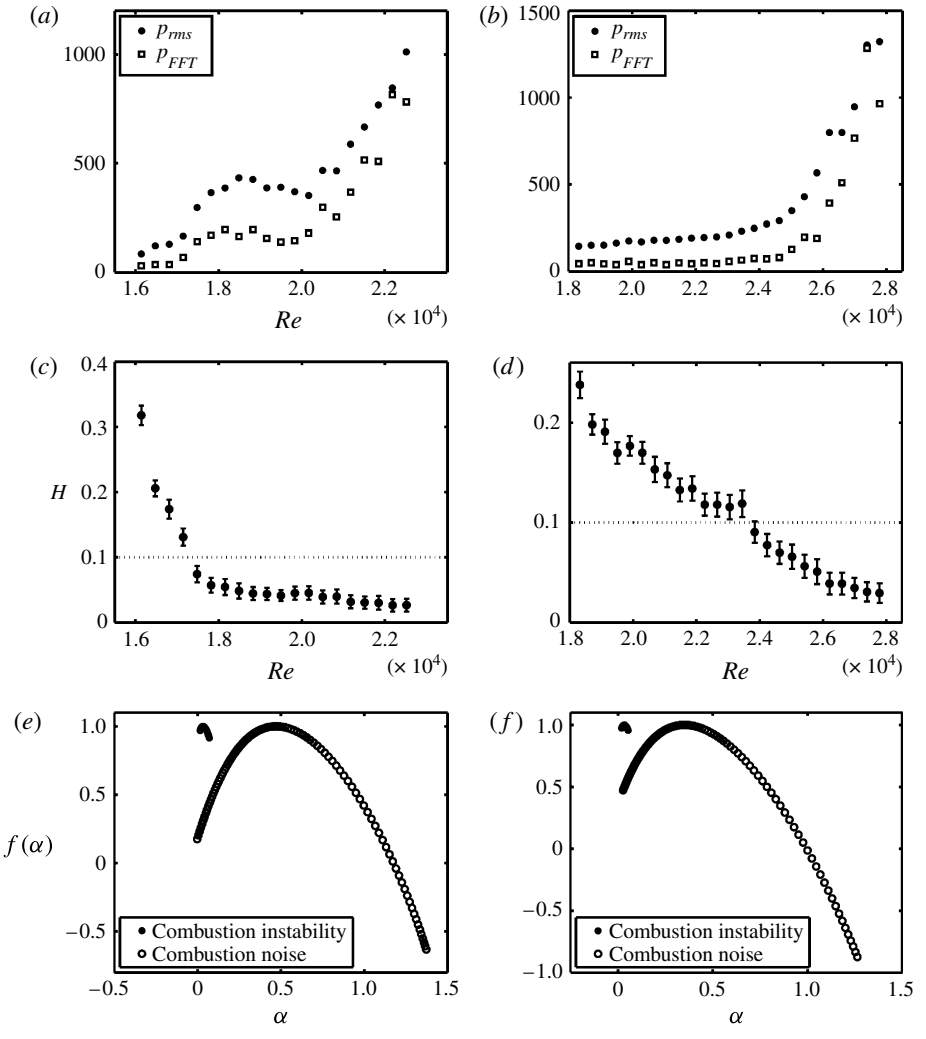

FIGURE 7. Variation of the amplitude of the pressure signals and the Hurst exponent H with Re for the two flameholding configurations of the combustor. The top row shows the r.m.s. levels of pressure fluctuations (p_{rms}) and the peak pressure amplitudes from the FFT (p_{FFT}) for the (a) swirl-stabilized configuration and (b) bluff-body-stabilized configuration. The corresponding variation in the Hurst exponent are shown in (c) and (d), respectively. The Hurst exponent drops well before the amplitude starts rising in the combustor. The error bars correspond to the 6–σ interval on the computed values. The threshold (shown as horizontal dotted lines) is nominally set to 0.1 to indicate the transition. This threshold is user-defined and is independent of the geometry of the system or the fuel composition, unlike the amplitude measurements. The loss of multifractality in the two configurations of the combustor is illustrated in (e) and (f), where the spectrum for the initial and final points shown in (c) and (d), respectively, is plotted. The time series from which the spectrum was obtained is the same as that shown in figure 2(b,d).

due to the predominance of a single time scale that dominates the dynamics. For a fractal signal, such a loss of variability in scales – observed as narrowing of the frequency spectrum – is termed a 'loss of spectral reserve' (West & Goldberger 1987).

In a combustor, since this loss of spectral reserve happens in a gradual manner when the parameters are varied, it can serve as an early warning signal to an impending combustion instability (Nair *et al.* 2012).

It should be noted that the flow is still turbulent after the combustor becomes unstable. The power spectrum (figure 2*f*) also shows that the contributions from time scales other than the instability frequencies and their multiples, though small, are still present. The effect of turbulence can also be seen in the modulation of the amplitude of pressure fluctuations at instability. It is this turbulence that results in a small range of α in the multifractal spectrum during combustion instability. However, the range of α is reduced significantly when compared to regimes of combustion noise, and is clustered around 0 for the instability dominated signals. A signal is multifractal when contributions of different time scales cannot be ignored without missing out on significant details of the phenomena. During combustion instability, it may be acceptable to consider the dynamics as a single time-scale problem. However, in the regions prior to instability, the contributions of other time scales cannot be ignored without missing key aspects of the dynamics. Also, ignoring the contributions of these time scales – as we have seen – results in the loss of predictability of an impending instability.

5. Concluding remarks

Traditional analysis and modelling of combustion noise, as well as that of combustion instability, often neglect or average out the unsteady irregular fluctuations observed in the measured data, or treat them as a stochastic background. A detailed analysis of the irregular fluctuations observed prior to the transition to combustion instability can be utilized to provide information that is of diagnostic as well as prognostic value. Combustion noise is deterministic chaos and results from the coupled nonlinear interaction amongst turbulence, combustion and the chamber acoustics. Hence, the use of the term noise to describe the pressure fluctuations inside a combustor during stable operation requires careful consideration, as the measurements do not display the features one would expect from a stochastic random process.

The pressure fluctuations during combustion noise further display multifractality which shows that multiple spatial/temporal scales contribute to its dynamics. The presence of multiple time scales also draws attention to the possibility of an inverse energy cascade in the inertial subrange which can possibly explain the formation of large-scale coherent structures at combustion instability. There is a gradual loss of multifractalilty for increases in Reynolds number towards combustion instability. Such a loss of spectral reserve acts as an early warning signal that predicts combustion instability well before the amplitudes start to rise in the combustor – in other words, well before the actual stability margins are reached. Moreover, the superiority of the method is clear on realizing that techniques such as FFT that rely on a frequency-domain analysis often cannot predict the proximity of the operating conditions to combustion instability.

Acknowledgements

We are grateful to the Department of Science and Technology, Government of India for partly funding this study. We express our gratitude to Professor Wolfgang Polifke and Mr Thomas Komarek of TU Munich, Germany for sharing the design of the combustor. We gratefully acknowledge the discussions with Mr Gireeshkumaran Thampi and the help received from Mr E. A. Gopalakrishnan and Mr R. Vishnu (all of IIT Madras) in performing the experiments.

Appendix A. Evaluation of generalized Hurst exponents and the multifractal spectrum

To estimate the Hurst exponent using DFA, the time signal $p(t)$ of length N is first mean-adjusted. Then a cumulative deviate series y_k is obtained as:

$$y_k = \sum_{t=1}^{k} (p(t) - m) \tag{A 1}$$

where

$$m = \frac{1}{N} \sum_{t=1}^{N} p(t). \tag{A 2}$$

The deviate series is further divided into a number n_w of non-overlapping segments $(y_i(t),\ i = 1, 2, \ldots, n_w)$ of equal span w. In order to remove the trends in the segments, a local linear fit $\bar{y}_i$ is made to the deviate series y_i and the fluctuations are obtained by subtracting the linear fit from the deviate series.

The structure function of order q and span w, F_w^q, can then be obtained from the fluctuations as:

$$F_w^q = \left(\frac{1}{n_w} \sum_{i=1}^{n_w} \left(\sqrt{\frac{1}{w} \sum_{t=1}^{w} (y_i(t) - \bar{y}_i)^2} \right)^q \right)^{1/q}. \tag{A 3}$$

For $q = 0$, the structure function is defined as Ihlen (2012):

$$F_w^0 = \exp\left(\frac{1}{2n_w} \sum_{i=1}^{n_w} \log\left(\frac{1}{w} \sum_{t=1}^{w} (y_i(t) - \bar{y}_i)^2 \right) \right). \tag{A 4}$$

The Hurst exponent H^2 (or H) is the slope of the linear regime on a logarithmic plot of F_w^2 for various span sizes w. Similarly, the generalized Hurst exponents H^q are the slopes of the linear regime on a logarithmic plot of F_w^q of various orders q, for variations in the segment width w. The information contained in H^q for different q can alternatively be represented as a spectrum of singularities $f(\alpha)$, which are related to H^q via a Legendre transform (Zia, Redish & McKay 2009).

$$\tau_q = qH^q - 1 \tag{A 5}$$

$$\alpha = \frac{\partial \tau_q}{\partial q} \tag{A 6}$$

$$f(\alpha) = q\alpha - \tau_q. \tag{A 7}$$

This spectrum, represented as a plot of $f(\alpha)$ against α, is known as the multifractal spectrum (also called the Hölder spectrum) and provides information on the various fractal scalings present in the data.

REFERENCES

BASSINGTHWAIGHTE, J. B., LIEBOVITCH, L. S. & WEST, B. J. 1994 *Fractal Physiology*. Oxford University Press.

BURNLEY, V. S. & CULICK, F. E. C. 2000 Influence of random excitations on acoustic instabilities in combustion chambers. *AIAA J.* **38**, 1403–1410.

CANDEL, S. 2002 Combustion dynamics and control: progress and challenges. *Proc. Combust. Inst.* **29**, 1–28.

CANDEL, S., DUROX, D., DUCRUIX, S., BIRBAUD, A.-L., NOIRAY, N. & SCHULLER, T. 2009 Flame dynamics and combustion noise: progress and challenges. *Intl J. Aeroacoust.* **8**, 1–56.

CHAKRAVARTHY, S. R., SHREENIVASAN, O. J., BOEHM, B., DREIZLER, A. & JANICKA, J. 2007 Experimental characterization of onset of acoustic instability in a nonpremixed half-dump combustor. *J. Acoust. Soc. Am.* **122**, 120–127.

CHAKRAVARTHY, S. R., SIVAKUMAR, R. & SHREENIVASAN, O. J. 2007 Vortex-acoustic lock-on in bluff-body and backward-facing step combustors. *Sadhana* **32**, 145–154.

CLAVIN, P., KIM, J. S. & WILLIAMS, F. A. 1994 Turbulence-induced noise effects on high-frequency combustion instabilities. *Combust. Sci. Technol.* **96**, 61–84.

COATS, C. M. 1996 Coherent structures in combustion. *Prog. Energy Combust. Sci.* **22**, 427–509.

CULICK, F. E. C. 2006 Unsteady motions in combustion chambers for propulsion systems. Vol. AG-AVT-039. RTO AGARDograph.

FRISCH, U. 1995 *Turbulence: The Legacy of A. N. Kolmogorov*. p. 66. Cambridge University Press.

FRISCH, U. & PARISI, G. 1985 On the singularity structure of fully developed turbulence. In *Turbulence and Predictability in Geophysical Fluid Dynamics* (ed. M. Gil., R. Benzi & G. Parisi), pp. 84–88. North-Holland.

GOTODA, H., AMANO, M., MIYANO, T., IKAWA, T., MAKI, K. & TACHIBANA, S. 2012 Characterization of complexities in combustion instability in a lean premixed gas-turbine model combustor. *Chaos* **22**, 043128.

GOTODA, H., NIKIMOTO, H., MIYANO, T. & TACHIBANA, S. 2011 Dynamic properties of combustion instability in a lean premixed gas-turbine combustor. *Chaos* **21**, 013124.

GOULDIN, F. C. 1987 An application of fractals to modeling premixed turbulent flames. *Combust. Flame* **68**, 249–266.

GOULDIN, F. C., BRAY, K. N. C. & CHEN, J. Y. 1989 Chemical closure model for fractal flamelets. *Combust. Flame* **77**, 241–259.

GOULDIN, F. C., HILTON, S. M. & LAMB, T. 1988 Experimental evaluation of the fractal geometry of flamelets. *Twenty-Second International Symp. on Combustion* 541–550.

HEGDE, U. G., REUTER, D., DANIEL, B. R. & ZINN, B. T. 1987 Flame driving of longitudinal instabilities in dump type ramjet combustors. *Combust. Sci. Technol.* **55**, 125–138.

HURST, H. E. 1951 Long-term storage capacity of reservoirs. *Trans. Am. Soc. Civil Engrs* **116**, 770–808.

IHLEN, E. A. 2012 Introduction to multifractal detrended fluctuation analysis in Matlab. *Front. Physiol.* **3**.

JEGADEESAN, V. & SUJITH, R. I. 2013 Experimental investigation of noise induced triggering in thermoacoustic systems. *Proc. Combust. Inst.* **34**, 3175–3183.

KANTELHARDT, J. W. 2011 Fractal and multifractal time series. In *Mathematics of Complexity and Dynamical Systems*, pp. 463–487. Springer.

KANTELHARDT, J. W., KOSCIELNY-BUNDE, E., REGO, H. H. A., HAVLIN, S. & BUNDE, A. 2001 Detecting long-range correlations with detrended fluctuation analysis. *Physica* A **295**, 441–454.

KANTELHARDT, J. W., ZSCHIEGNER, S. A., KOSCIELNY-BUNDE, E., HAVLIN, S., BUNDE, A. & STANLEY, H. E. 2002 Multifractal detrended fluctuation analysis of nonstationary time series. *Physica* A **316**, 87–114.

KAPLAN, D. T. & GLASS, L. 1992 Direct test for determinism in a time series. *Phys. Rev. Lett.* **68**, 427–430.

KOLMOGOROV, A. N. 1941 Dissipation of energy in the locally isotropic turbulence. *Dokl. Akad. Nauk SSSR* **32**, 16–18 (in Russian). Translated into English by Kolmogorov, A. N. Proceedings: Mathematical and Physical Sciences Vol. 434, No. 1890, Turbulence and Stochastic Process: Kolmogorov's Ideas 50 Years On (Jul. 8, 1991) , pp. 15–17.

KOMAREK, T. & POLIFKE, W. 2010 Impact of swirl fluctuations on the flame response of a perfectly premixed swirl burner. *Trans. ASME: J. Engng Gas Turbines Power* **132**, 061503.

KRAICHNAN, R. H. 1967 Inertial ranges in two-dimensional turbulence. *Phys. Fluids* **10**, 1417–1423.

LIEUWEN, T. C. 2001 Phase drift characteristics of self-excited, combustion driven oscillations. *J. Sound Vib.* **242**, 893–905.

LIEUWEN, T. C. 2002 Experimental investigation of limit-cycle oscillations in an unstable gas turbine combustor. *J. Propul. Power* **18**, 61–67.

LIEUWEN, T. C. 2003 Statistical characteristics of pressure oscillations in a premixed combustor. *J. Sound Vib.* **260**, 3–17.

LIEUWEN, T. 2005 Online combustor stability margin assessment using dynamic pressure data. *J. Engg. Gas Turbines Power* **127**, 478–482.

LIEUWEN, T. & BANASZUK, A. 2005 Background noise effects on combustor stability. *J. Propul. Power* **21**, 25–31.

LIEUWEN, T. C. & YANG, V. (ed.) 2005 *Combustion Instabilities in Gas Turbine Engines: Operational Experience, Fundamental Mechanisms, and Modeling*, vol. 210, AIAA Inc.

MANDELBROT, B. B. 1974 Intermittent turbulence in self-similar cascades: divergence of high moments and dimension of the carrier. *J. Fluid Mech.* **62**, 331–358.

MANDELBROT, B. B. 1982 *The Fractal Geometry of Nature*. W. H. Freeman and Company.

MASSEY, F. J. 1951 The Kolmogorov–Smirnov test for goodness of fit. *J. Am. Stat. Assoc.* **46**, 68–78.

MCMANUS, K. R., POINSOT, T. & CANDEL, S. M. 1993 A review of active control of combustion instabilities. *Prog. Energy Combust. Sci.* **16**, 1–29.

MENEVEAU, C. & SREENIVASAN, K. R. 1987 The multifractal spectrum of the dissipation field in turbulent flows. *Nucl. Phys. B Proc. Suppl.* **2**, 49–76.

MENEVEAU, C. & SREENIVASAN, K. R. 1989 Measurement of $f(\alpha)$ from scaling of histograms and applications to dynamical systems and fully developed turbulence. *Phys. Lett.* A **137**, 103–112.

MENEVEAU, C. & SREENIVASAN, K. R. 1991 The multifractal nature of turbulent energy dissipation. *J. Fluid Mech.* **224**, 429–484.

MONTROLL, E. W. & SCHLESINGER, M. F. 1982 On $1/f$ noise and other distributions with long tails. *Proc. Natl Acad. Sci. USA* **79**, 3380–3383.

NAIR, V. & SUJITH, R. I. 2013 Identifying homoclinic orbits in the dynamics of intermittent signals through recurrence quantification. *Chaos* **23**, 033136.

NAIR, V., THAMPI, G., KARUPPUSAMY, S., GOPALAN, S. & SUJITH, R. I. 2013 Loss of chaos in combustion noise as a precursor of impending combustion instability. *Intl J. Spray Combust. Dyn.* **5**, 273–290.

NAIR, V., THAMPI, G., SULOCHANA, K., SARAVANAN, G. & SUJITH, R. I. 2012 System and method for predetermining the onset of impending oscillatory instabilities in practical devices, Provisional Patent, Filed October 26.

NOIRAY, N. & SCHUERMANS, B. 2013 Deterministic quantities characterizing noise driven Hopf bifurcations in gas turbine combustors. *Intl J. Non-Linear Mech.* **50**, 152–163.

PALADIN, G. & VULPIANI, A. 1987 Anomalous scaling laws in multifractal objects. *Phys. Rep.* **156**, 147–225.

PARKER, L. J., SAWYER, R. F. & GANJI, A. R. 1979 Measurement of vortex frequencies in a lean, premixed prevaporized combustor. *Combust. Sci. Technol.* **20**, 235–241.

PENG, C.-K., BULDYREV, S. V., HAVLIN, S., SIMONS, M., STANLEY, H. E. & GOLDBERGER, A. L. 1994 Mosaic organization of DNA nucleotides. *Phys. Rev.* E **49**, 1685–1689.

PIKOVSKY, A., ROSENBLUM, M. & KURTHS, J. 2001 *Synchronization: A Universal Concept in Nonlinear Sciences*. p. 38. Cambridge University Press.

PITZ, R. W. & DAILY, J. W. 1983 Combustion in a turbulent mixing layer formed at a rearward-facing step. *AIAA J.* **21**, 1565–1570.

POINSOT, T. J., TROUVE, A. C., VEYNANTE, D. P., CANDEL, S. M. & ESPOSITO, E. J. 1987 Vortex-driven acoustically coupled combustion instabilities. *J. Fluid Mech.* **177**, 265–292.

PRASAD, R. R., MENEVEAU, C. & SREENIVASAN, K. R. 1988 The multifractal nature of the dissipation field of passive scalars in fully turbulent flows. *Phys. Rev. Lett.* **61**, 74–77.

RAYLEIGH, J. W. S. 1878 The explanation of certain acoustical phenomena. *Nature* **18**, 319–321.

RICHARDSON, L. F. 1922 *Weather Prediction by Numerical Process*. Cambridge University Press.

ROGERS, D. E. & MARBLE, F. E. 1956 A mechanism for high-frequency oscillation in ramjet combustors and afterburners. *Jet Propul.* **26**, 456–462.

SCHADOW, K. C. & GUTMARK, E. 1992 Combustion instability related to vortex shedding in dump combustors and their passive control. *Prog. Energy Combust. Sci.* **18**, 117–132.

SCHLESINGER, M. F. 1987 Fractal time and $1/f$ noise in complex systems. *Ann. N.Y. Acad. Sci.* **504**, 214–228.

SCHWARZ, A. & JANICKA, J. (ed.) 2009 *Combustion Noise*. Springer.

SMITH, D. A. & ZUKOSKI, E. E. 1985 Combustion instability sustained by unsteady vortex combustion. In *AIAA/SAE/ASME/ASEE 21st Joint Propulsion Conference. Monterey, California*.

SREENIVASAN, K. R. 1991 Fractals and multifractals in fluid turbulence. *Annu. Rev. Fluid Mech.* **23**, 539–604.

SREENIVASAN, K. R. & MENEVEAU, C. 1986 The fractal facets of turbulence. *J. Fluid Mech.* **173**, 357–386.

SREENIVASAN, K. R. & MENEVEAU, C. 1988 Singularities of the equations of fluid motion. *Phys. Rev.* A **38**, 6287–6295.

STRAHLE, W. C. 1978 Combustion noise. *Prog. Energy Combust. Sci.* **4**, 157–176.

STRAHLE, W. C. & JAGODA, J. I. 1988 Fractal geometry applications in turbulent combustion data analysis. *Twenty-Second Symp. on Combustion* 561–568.

SUROVYATKINA, E. 2005 Prebifurcation noise amplification and noise-dependent hysteresis as indicators of bifurcations in nonlinear geophysical systems. *Nonlinear Process. Geophys.* **12**, 25–29.

TAYLOR, G. I. 1938 The spectrum of turbulence. *Proc. R. Soc. Lond.* A **164**, 476–490.

WEST, B. J. 2006 *Where Medicine Went Wrong: Rediscovering the Path to Complexity*. p. 55. World Scientific.

WEST, B. J. & GOLDBERGER, A. L. 1987 Physiology in fractal dimensions. *Am. Sci.* **75**, 354–365.

WEST, B. J., LATKA, M., GLAUBIC-LATKA, M. & LATKA, D. 2003 Multifractality of cerebral blood flow. *Physica* A **318**, 453–460.

WIESENFELD, K. 1985 Noisy precursors of nonlinear instabilities. *J. Stat. Phys.* **38**, 1071–1097.

WILKE, C. R. 1950 A viscosity equation for gas mixtures. *J. Chem. Phys.* **18**, 517–519.

WINANT, C. D. & BROWAND, F. K. 1974 Vortex pairing: the mechanism of turbulent mixing-layer growth at moderate Reynolds numbers. *J. Fluid Mech.* **63**, 237–255.

YU, K. H., TROUVE, A. & DAILY, J. W. 1991 Low-frequency pressure oscillations in a model ramjet combustor. *J. Fluid Mech.* **232**, 47–72.

ZANK, G. P. & MATTHAEUS, W. H. 1990 Nearly incompressible hydrodynamics and heat conduction. *Phys. Rev. Lett.* **64**, 1243–1246.

ZIA, R. K., REDISH, E. F. & MCKAY, S. R. 2009 Making sense of the Legendre transform. *Am. J. Phys.* **77**, 614–622.